0.6-eV bandgap $In_{0.69}Ga_{0.31}As$ thermophotovoltaic devices with compositionally undulating step-graded $InAsyP_{1-y}$buffers*

Ji Lian(季 莲)[a], Lu Shu-Long(陆书龙)[a]†, Jiang De-Sheng(江德生)[b], Zhao Yong-Ming(赵勇明)[a], Tan Ming(谭 明)[a], Zhu Ya-Qi(朱亚棋)[a], and Dong Jian-Rong(董建荣)[a]

[a] *Key Laboratory of Nanodevices and Applications, Suzhou Institute of Nano-tech and Nano-bionics, Chinese Academy of Sciences, Suzhou* 215125, *China*
[b] *State Key Laboratory of Integrated Optoelectronics, Institute of Semiconductors, Chinese Academy of Sciences, P O Box* 912, *Beijing* 100083, *China*

(Received 9 June 2012; revised manuscript received 17 July 2012)

Single-junction, lattice-mismatched $In_{0.69}Ga_{0.31}As$ thermophotovoltaic (TPV) devices each with a bandgap of 0.6 eV are grown on InP substrate by metal–organic chemical vapour deposition (MOCVD). Compositionally undulating step-graded $InAs_yP_{1-y}$ buffer layers with a lattice mismatch of ∼1.2% are used to mitigate the effect of lattice mismatch between the device layers and the InP substrate. With an optimized buffer thickness, the $In_{0.69}Ga_{0.31}As$ active layers grown on the buffer display a high crystal quality with no measurable tetragonal distortion. High-performance single-junction devices are demonstrated, with an open-circuit voltage of 0.215 V and a photovoltaic conversion efficiency of 6.9% at a short-circuit current density of 47.6 mA/cm^2, which are measured under the standard solar simulator of air mass 1.5-global (AM 1.5 G).

Keywords: $In_{0.69}Ga_{0.39}As$, thermophotovoltaic devices, $InAs_yP_{1-y}$ buffer

PACS: 68.55.ag, 81.15.Gh, 88.40.hj, 88.40.jm **DOI:** 10.1088/1674-1056/22/2/026802

1. Introduction

$In_xGa_{1-x}As$-based thermophotovoltaic (TPV) devices grown on InP substrates are of interest for a variety of terrestrial and space energy conversion applications.[1–4] Most TPV systems are designed to generate electricity from thermal sources that operate in a temperature range from 1000 K to 2000 K, which require $In_xGa_{1-x}As$ TPV cells with bandgaps from 0.5 eV to 0.74 eV. To achieve the desired bandgap values, $In_xGa_{1-x}As$ (with $x > 0.53$) can be grown into lattice-mismatched structures on an InP substrate with an $InAs_yP_{1-y}$ buffer to mitigate the lattice mismatch.[5–11] To date, all reported $In_xGa_{1-x}As$-based TPV devices have been grown using a compositionally monotonically graded $InAs_yP_{1-y}$ buffer. Compared with more common compositionally monotonically graded buffer choices, compositionally non-monotonically graded buffers offer an additional degree of freedom for tailoring the shape of the misfit profile. In this work, lattice mismatched $In_{0.69}Ga_{0.31}As$ (0.6 eV) TPV devices with compositionally undulating step-graded $InAs_yP_{1-y}$ buffers grown by metal–organic chemical vapour deposition (MOCVD) on InP are studied. High quality $In_{0.69}Ga_{0.31}As$ material and high performance devices are demonstrated for a bandgap of 0.6 eV.

2. MOCVD growth and device processing

Lattice-mismatched $In_{0.69}Ga_{0.31}As$ TPV structures were grown by a horizontal low-pressure MOCVD system on n-doped (100) InP substrates, using trimethylgallium and trimethylindium as the group III sources, AsH_3 and PH_3 as the group V sources, silane (SiH4) as n-type dopant, DEZn as p-type dopant, and palladium diffused H_2 as the carrier gas. An initial 50-nm thick n-doped InP buffer layer was deposited to generate a smooth surface. After InP growth, the $InAs_yP_{1-y}$ buffer layer was grown at a nominal rate of 2.5 Å/s (1 Å=0.1 nm) and at a constant substrate temperature of 680 °C under stabilized phosphorus flux with variable As flux, in order to provide a nearly lattice-matched "virtual" substrate for the further overgrowth of 0.6-eV $In_xGa_{1-x}As$ ($x \approx 0.68$) TPV active layers. In the $InAs_yP_{1-y}$ buffer layer, the As composition increased in an undulating manner, i.e., with a high As composition followed by a low As composition and then a higher As composition again, so as to form an alternate growth of compressive strain and tensile strain material. The extent of lattice misfit between the desired InGaAs active layer and the InP substrate was 1.0%. It is noted that in order to compensate the residual stain, the grown uppermost $InAs_yP_{1-y}$ buffer layer should intentionally have a lattice misfit extent of 1.2% with respect to InP, which is a little bit higher than that for $In_{0.69}Ga_{0.31}As$, which will be discussed in more detail later. For comparison, two samples, A and B, were grown and they had similar buffer structures except for their layer thickness. The total buffer thicknesses for sample A and sample B are 1.5 μm and 2.2 μm, respectively. Accurate determination of the As mole-fraction was obtained from triple axis X-ray diffraction (XRD) measurements, which allowed the calculation of the residual strain remaining in the

*Project supported by the National Basic Research Program of China (Grant No. 61176128), the Knowledge Innovation Project of the Chinese Academy of Sciences, and Suzhou Municipal Solar Cell Research Project, China (Grant No. SYG201145).

†Corresponding author. E-mail: sllu2008@sinano.ac.cn

© 2013 Chinese Physical Society and IOP Publishing Ltd

layers. Full details related to the growth and properties of the $InAs_yP_{1-y}$ buffer are reported elsewhere.[12]

The schematic cross section of a basic n–p–n TPV structure is shown in Fig. 1 which allows the use of the desired n-on-p cell configuration with an InGaAs tunnel junction as needed for monolithic interconnected module (MIM) TPV.[13] The active region of the cell consists of a p/n junction (base/emitter) of InGaAs surrounded by the layers of InAsP, which is used to passivate the high recombination-velocity InGaAs surface and confine the minority carriers, leading to an improved device performance.[14] The Ni/AuGe/Ni/Au metallization was used for the n-type Ohmic contact. An anti-reflection coating (ARC) of SiO_2/TiO_2 was deposited on the top surface. For comparison, a lattice-matched $In_{0.53}Ga_{0.47}As$ TPV device (sample C) with a bandgap of 0.73 eV was fabricated, which had the same structure as samples A and B except for no InAsP buffer layers. The size of each of the cell devices is 2.5 mm×2.5 mm.

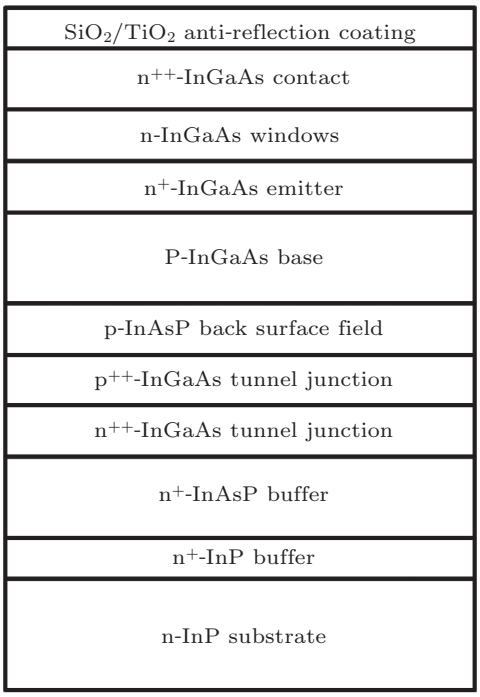


Fig. 1. Cross section of the double heterostructure (InGaAs/InAsP) 0.6 eV TPV device grown on n-InP substrate.

3. Material characteristics

The relaxation state and residual strain of the samples were checked by reciprocal space maps (RSMs) with asymmetric (115) reflection measured using high-resolution triple axis XRD as shown in Fig. 2. For sample A, the (115) RSM exhibits only two distinct reciprocal lattice point (RLP) maxima, one is for the substrate and the other is for the $In_{0.69}Ga_{0.31}As$ layer, as shown in Fig. 2(a). The RLP of $In_{0.69}Ga_{0.31}As$ layer exhibits a larger peak broadening compared with sample B, which is attributed to higher dislocation density and poorer crystal quality of sample A as confirmed by TEM analysis. For sample B, there are three distinct RLP maxima in the RSM, and the peaks corresponding to these RLP maxima are assigned to (i) the InP substrate, (ii) the uppermost $InAs_yP_{1-y}$ buffer layer, and (iii) the $In_{0.69}Ga_{0.31}As$ cover layer. The $In_{0.69}Ga_{0.31}As$ layer RLP lies directly on the uppermost $InAs_yP_{1-y}$ buffer layer, so its in-plane lattice constant is coherent with that of the uppermost $InAs_yP_{1-y}$ layer, indicating that the internal lattice matching has been achieved between the $In_{0.69}Ga_{0.31}As$ layer and the $InAs_yP_{1-y}$ layer. In addition, the $In_{0.69}Ga_{0.31}As$ layer RLP is exactly centred on the line extending between the substrate RLP and $Q = 0$, indicating that the $In_{0.69}Ga_{0.31}As$ has reached their equilibrium cubic structure with no measurable tetragonal distortion, which is attributed to the fact that the uppermost $InAs_yP_{1-y}$ buffer layer is grown up to a composition corresponding to a lattice constant of $a_s = a_1 + \varepsilon a_0$, overshooting the desired device lattice constant by a small amount εa_0,[15] where a_0 corresponds to InP lattice constant, a_1 corresponds to the lattice constant of $In_{0.69}Ga_{0.31}As$, and ε corresponds to residual strain at the surface of the buffer layer.

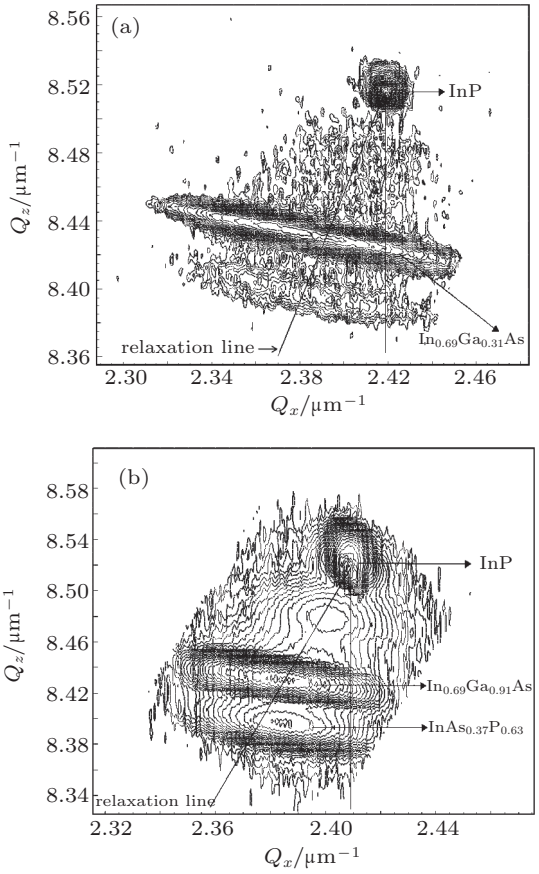


Fig. 2. Asymmetric (115) RSMs of the $In_{0.69}Ga_{0.31}As$ TPV device epitaxial layers grown on (001) InP substrate for (a) sample A, (b) sample B.

According to the atomic force microscopy (AFM) measurements (not shown here), the expected crosshatch morphology that is characteristic of strain relaxation induced by

the growth with $InAs_yP_{1-y}$ buffers is evident. The root-mean-square (RMS) roughness of sample A is 14 nm (the scan area is 20 μm×20 μm), which is much larger than 1.44 nm of sample B. The obtained results indicate that the thickness of the $InAs_yP_{1-y}$ buffer layer has a great influence on $In_{0.69}Ga_{0.31}As$ crystal quality and surface morphology. The smallest RMS roughness for our compositionally undulating $InAs_yP_{1-y}$ buffer case is 2.74 nm (the scan area is 40 μm×40 μm), small as compared with 3.6 nm reported for the step-like grading $InAs_yP_{1-y}$ buffer grown by molecular beam epitaxy,[16] which is attributed to the advantages of alternate growth of compressive strain and tensile strain material.

4. Device characteristics

The current–voltage (I–V) characteristic curves of lattice-matched (sample C) and lattice-mismatched (sample A and sample B) TPV devices under the standard solar simulator of air mass 1.5-global (AM 1.5G) are shown in Fig. 3. It is obvious that the short-circuit current density of the mismatched TPV device is larger than that of the matched TPV device due to the lower InGaAs bandgap. The calibration at 1 sun shows that the lattice-mismatched cell sample A has a photovoltaic conversion efficiency of 5.31% with an open voltage (V_{oc}) of 0.19 V, a short-circuit current density (J_{sc}) value of 43 mA/cm^2, and a fill factor (FF) of 58%. The lattice-mismatched cell sample B has a better photovoltaic conversion efficiency (6.9%) with a higher V_{oc} (0.215 V), a larger J_{sc} value (47.6 mA/cm^2), and an FF of 57%. The optoelectronic operation of the solar cell device includes the process of photon absorption, carrier separation, transport, and collection. Therefore, many parameters may affect the performance of the device. However, if only the material quality is considered, we need to increase the diffusion length of minority carriers and reduce the recombination, such as surface recombination, defect-state-related recombination, etc. However, in order to optimize the above factors, the most important thing is to lower the defect density. Aforementioned XRD analyses indicate that the crystal quality of sample B is better than that of sample A, which is consistent with the I–V characteristics result.

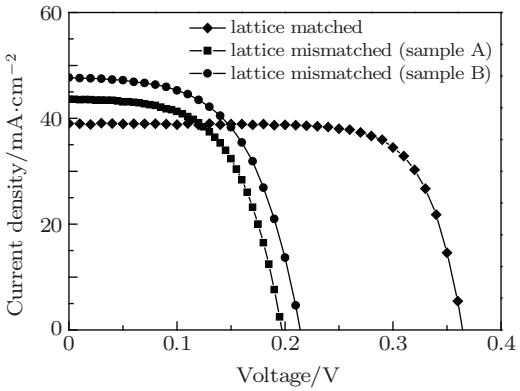


Fig. 3. Current–voltage (I–V) characteristic curves of lattice-matched and lattice-mismatched TPV devices.

The results of external quantum efficiency (EQE) of lattice-matched and lattice-mismatched TPV devices are shown in Fig. 4. Because of the limitations of our test system, the measured wavelengths range from 0.9 μm to 1.9 μm. For the lattice-matched sample C, the EQE value is high, which is ∼ 90% falling in an interval between wavelengths 1.0 μm and 1.67 μm, which is consistent with a long carrier diffusion length. In addition, a sharp band edge cutoff is observed. The lattice-mismatched cell has a poor EQE property compared with the lattice-matched TPV device. For sample A, the EQE value keeps low in the measurement range, indicating a small diffusion length of minority carriers due to the poor material quality. For sample B, the EQE value is low at short wavelength and it increases as wavelength increases. The highest value is ∼ 90%. A similar spectral dependence of the EQE property was reported and was attributed to the front surface recombination since a substantial amount of absorption at short wavelengths takes place close to the emitter surface.[17] According to the simulation results, the EQE at short wavelength decreases dramatically when front surface recombination velocity, S_f, is larger than 10^5 cm/s, whereas it is nearly constant for $S_f < 2 \times 10^3$ cm/s.

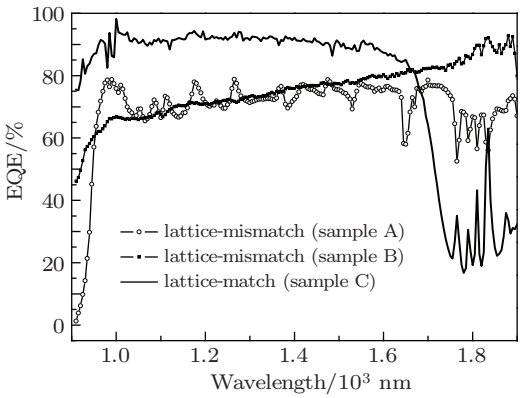


Fig. 4. Curves of external quantum efficiency (EQE) versus wavelength of lattice-matched and lattice-mismatched TPV devices.

5. Conclusion

Lattice-mismatched $In_{0.69}Ga_{0.31}As$ thermophotovoltaic (TPV) devices with compositionally undulating step-graded $InAs_yP_{1-y}$ buffers are fabricated and tested. With the advantages of alternate growth of compressive strain and tensile strain material, the $In_{0.69}Ga_{0.31}As$ active layer which shows a high crystal quality (with no measurable tetragonal distortion) and a very low surface roughness of 2.74 nm is obtained. High-performance devices are obtained, with the single-junction one displaying a V_{oc} of 0.215 V and an FF of 57% measured at a J_{sc} value of 47.6 mA/cm^2. The results suggest great promise for achieving high efficiency, large area,

low bandgap InGaAs TPV modules and arrays by using compositionally undulating step-graded $InAs_yP_{1-y}$ buffers.

References

[1] Hudait M K, Andre C L, Kwon O, Palmisiano M N and Ringel S A 2002 *IEEE Electron. Dev. Lett.* **23** 697

[2] Wanlass M W, Ward J S, Emery K A, Al-Jassim M M, Jones K M and Coutts T J 1996 *Sol. Energy Mater. Sol. Cell* **41** 405

[3] Wanlass M W, Carapella J J, Duda A, Emery K, Gedvilas L, Moriarty T, Ward S, Webb J D and Wu X 1999 *Proc. NREL Conf. TPV Generation Electricity (AIP)* **460** 132

[4] Hudait M K, Lin Y, Palmisiano M N and Ringel S A 2003 *IEEE Electron. Dev. Lett.* **24** 538

[5] Beaudoin M, Bensaada A, Leonelli R, Desjardins P, Masut R A, Isnard L, Chennouf A and L'Esperance G 1996 *Phys. Rev.* B **53** 1990

[6] Okada T, Kruzelecky R V, Weatherly G C, Thompson D A and Robinson J B 1993 *Appl. Phys. Lett.* **63** 3194

[7] Hudait M K, Lin Y and Ringel S A 2009 *J. Appl. Phys.* **105** 061643

[8] Hudait M K, Lin Y, Palmisiano M N, Tivarus C, Pelz J P and Ringel S A 2004 *J. Appl. Phys.* **95** 3952

[9] Ahrenkiel S P, Wanlass M W, Carapella J J, Ahrenkiel P K, Johnston S W and Gedvials L M 2007 *Sol. Energy Mater. Sol. Cell* **91** 908

[10] Gao H L, Zeng Y P and Wang B Q 2008 *Chin. Phys.* B **17** 1119

[11] Xu J B, Zhang H Y, Fu X J, Guo T Y and Huang J E 2010 *Chin. Phys.* B **19** 037302

[12] Ji L, Lu S L, Zhao Y M, Tan M, Zhu Y Q and Dong J R "Compositionally Undulating Step-graded $InAs_yP_{1-y}$ Buffer Layer Growth by Metal–organic Chemical Vapor Deposition", to be published in *J. Crys. Growth*

[13] Fatemi N S, Wilt D M, Hoffman R W, Stan M A, Weizer V G, Jenkins P P, Khan O S, Murray C S, Scheiman D and Brinker D 1999 *Proc. NREL Conf. TPV Generation Electricity (AIP)* **460** 121

[14] Siergiej R R, Wersman B, Derry S A, Mahorter R G, Wehrer R J, Link S D, Palmisiano M N, Messham R L, Murray S, Murray C S, Newman F, Hills J and Taylor D 2003 *Proc. NREL Conf. TPV Generation Electricity (AIP)* **653** 414

[15] Tersoff J 1993 *Appl. Phys. Lett.* **62** 693

[16] Hudait M K, Lin Y, Speck J S, Tivarus C A, Heller E R, Pelz J P and Ringel S A 2003 *Appl. Phys. Lett.* **82** 3212

[17] Su N, Fay P, Sinharoy S, Forbes D and Scheiman D 2007 *J. Appl. Phys.* **101** 064511